

©2016, Elsevier. Licensed under the Creative Commons Attribution-NonCommercial-NoDerivatives 4.0 International <http://creativecommons.org/about/downloads>



1 **Authors' affiliations**

2

3 Natalja Petkune, PhD student, Department of Civil Engineering, Kingston University London,

4 Surrey, KT1 2EE, UK, Email: N.Petkune@kingston.ac.uk

5

6 Ted Donchev, Associate Professor, Department of Civil Engineering, Kingston University

7 London, Surrey, KT1 2EE, UK, Email: T.Donchev@kingston.ac.uk

8

9 Homayoun Hadavinia, Associate Professor, School of Mechanical & Automotive Engineering,

10 Kingston University London, SW15 3DW, UK, Email: H.Hadavinia@kingston.ac.uk

11

12 David Wertheim, Professor, Faculty of Science, Engineering and Computing, Kingston

13 University London, Surrey, KT1 2EE, UK, Email: D.Wertheim@kingston.ac.uk

14

15 Mukesh Limbachiya, Professor, Department of Civil Engineering, Kingston University

16 London, Surrey, KT1 2EE, UK, Email: M.Limbachiya@kingston.ac.uk

17

18 **Performance of pristine and retrofitted hybrid steel / fibre reinforced polymer**
19 **composite shear walls**

20

21 Natalja Petkune^{1*}, Ted Donchev^{1*}, Homayoun Hadavinia², Mukesh
22 Limbachiya¹, David Wertheim³

23

24 ¹ Department of Civil Engineering, Kingston University London, KT1 2EE, UK

25 ² School of Mech & Auto Engineering, Kingston University London, SW15 3DW, UK

26 ³ Faculty of Science, Engineering and Computing, Kingston University London, KT1 2EE, UK

27

28 **ABSTRACT**

29 In this study new types of advanced hybrid shear wall systems using steel/fibre reinforced
30 polymer (FRP) composites are being developed for deployment in the construction of
31 buildings. The hybrid steel/FRP shear walls made from laminates of steel with either carbon
32 FRP (CFRP) or glass FRP (GFRP) materials. In total six medium-scaled shear wall
33 specimens were manufactured. In the first phase of the study three pristine specimens: steel
34 shear wall (SSW-P), hybrid steel /CFRP shear wall (HSCSW-P) and hybrid steel/GFRP
35 shear wall (HSGSW-P) were tested. In the second phase of the project, the specimens
36 tested in phase one were retrofitted and retested; these specimens were identified as SSW-
37 R, HSCSW-R and HSGSW-R. The structural repair and strengthening of specimens in the
38 second phase was achieved by replacing the damaged infill plates with new infill plates of the
39 same type, strengthening of the vertical steel frame elements with CFRP laminates and
40 GFRP fabric. All shear wall specimens were tested under quasi-static cyclic loading following
41 the ATC-24 protocol. The behaviour and failure modes of the pristine and retrofitted
42 specimens were compared. The results show that the retrofitted specimens with the

* Corresponding authors: Emails: N.Petkune@kingston.ac.uk (Natalja Petkune),
T.Donchev@kingston.ac.uk (Ted Donchev)

43 procedure developed have higher stiffness, higher ultimate loading capacity and similar
44 energy dissipation capability relative to pristine specimens. For hybrid retrofitted specimens
45 the ultimate load capacity increased more than 11% in comparison with pristine hybrid
46 specimens.

47 **Keywords:** Steel and hybrid shear wall; Fibre reinforced polymer composite; Medium scale
48 shear wall specimens; earthquake loading; retrofitting.

49 **1 INTRODUCTION**

50 Steel shear walls (SSW), consisting of steel boundary elements and steel infill plate, have
51 good lateral resisting properties and hence they can be used in regions with high levels of
52 seismic activity. Their benefits such as lightweight, high load bearing capacity and high
53 energy dissipation make them an attractive alternative in the construction of high-rise
54 buildings particularly in areas of seismic activity. However, one of the main problems limiting
55 their practical application is difficulty in repairing them after an earthquake event. Since the
56 1970s, SSWs have been popular in the USA and Japan for construction of high-rise
57 buildings; they provide significant reduction in wall thickness as well as weight of the building
58 and as a result reduction of foundation and inertia loads [1]. Hybrid shear walls (HSW)
59 consisting of steel boundary elements and steel infill plates laminated with fibre reinforced
60 polymers (FRP) on both sides of the plate are in process of the development. The
61 established definition for steel shear walls is a combination of the steel frame with steel infill
62 plate (e.g. see [1, 2, 3] to name a few). In this research the existing definition of steel shear
63 walls was further developed as hybrid shear walls for elements consisting of steel frames
64 and hybrid steel/FRP infill plates in aspect of infill plate modifications.

65 When buildings are subjected to seismic loading, severe damage to shear walls can
66 occur. It is important to use effective techniques to recover initial strength and stiffness of the
67 shear walls in order to avoid demolition of the building or requirement for introduction of new
68 additional elements. This paper will address the use of the fibre reinforced polymer
69 composites for enhancing the performance of SSW and also for a permanent retrofitting and
70 strengthening of steel and hybrid (steel/FRP) shear walls after earthquake damage. These
71 strengthening methods could also be applied to undamaged structures when changes in the
72 structural loads on an existing building require design of higher capacity SSWs or HSWs.

73

74

75 **2 BACKGROUND**

76 FRP materials have been used in civil engineering over several decades for
77 strengthening of reinforced concrete and steel structures, improving capacity of buildings,
78 bridges, dams and other structures. The most common FRP materials used for strengthening
79 purposes are glass FRP (GFRP) and carbon FRP (CFRP). The high tensile strength of FRP
80 and ease of application provides a clear benefit for their use in strengthening of structures.
81 Advantages of FRP over steel as a strengthening material include higher strength-to-weight
82 and stiffness-to-weight ratios, corrosion resistance, ease and speed of transportation and
83 installation, electromagnetic neutrality and ability to follow irregular shapes of structures via
84 wet lay-up- processes.

85 **2.1 FRP strengthening of steel structures**

86 Strengthening of steel structures with FRP in comparison with strengthening steel
87 members by welding additional steel plates can be particularly beneficial in applications
88 where it is important to avoid new residual stresses caused by the welding process and to
89 avoid local strength reductions in heat affected zones [4].

90 Review of the current applications of steel structures strengthened with FRP by Teng
91 et al. [5] and Zhao and Zhang [6] highlighted that the behaviour of the steel/FRP structural
92 elements depends on the selection of the adhesive with appropriate mechanical properties
93 not only in short-term performance, but also in long-term durability. It is important for bond-
94 critical applications to use appropriate preparation techniques of the steel surfaces before
95 adhesive application.

96 The main area of applications of using FRP for strengthening of steel structures can
97 be summarised in the following categories:

- 98 • strengthening of steel elements against local buckling [7, 8]
- 99 • flexural strengthening of the steel beams [9]
- 100 • fatigue strengthening for steel beams, steel plates and connections [10, 11]
- 101 • strengthening of steel hollow sections and concrete filled steel tubes [12, 13]

102 Harries et al. [7] conducted experiments on retrofitting columns made of WT steel
103 sections with ultra-high modulus of elasticity GFRP strips, which were tested under
104 concentric cyclic compressive loading to failure. Application of the FRP material prior to the
105 test resulted in delay of the plastic buckling and formation of the plastic “kink” which
106 positively affects energy dissipation and ultimate cyclic ductility properties. Similar
107 conclusions were made by El-Tawil et al. [8]. They investigated the behaviour of three double
108 channel built-up members wrapped with CFRP in the regions of plastic hinges tested under
109 cyclic loading. It was concluded that structural behaviour of CFRP reinforced specimens was
110 considerably better than unreinforced ones. CFRP wrapping in the regions of plastic hinges
111 increased the size of the plastic hinge region and slowed down the occurrence of the local
112 buckling. It also delayed the onset of lateral torsional buckling and resulted in a higher
113 energy dissipation capacity in the plastic hinge regions.

114 **2.2 FRP and steel applications for improving seismic resistance**

115 An important aspect for the use of the FRP is to improve seismic resistance of the
116 existing lateral load resisting system of buildings, particularly for shear walls. Several
117 experimental and numerical studies have been conducted to investigate the behaviour of
118 undamaged steel shear walls [14, 15, 16].

119 An innovative lateral resisting system in the form of hybrid shear walls (HSW),
120 consisting of steel frames and steel infill plates laminated with FRP, have been investigated
121 by several researchers in the past five years [3, 17, 18, 19, 20]. Experimental studies on the
122 use of hybrid steel/GFRP shear walls showed that they provide higher stiffness, larger
123 energy dissipation capacity and more uniform tension field during loading than steel shear
124 walls with the same thickness of the steel infill plate [17]. Nateghi et al. [18] tested steel
125 shear walls with infill plates laminated with GFRP, reaching a similar conclusion to Maleki et
126 al. [17] that it significantly increases ultimate strength and initial stiffness. Cumulative energy
127 dissipation of the hybrid steel/GFRP shear walls was larger than steel shear walls. Both

128 studies concluded that the fibre orientation plays a significant role in the behaviour of the
129 specimens, and laminates with fibres in the direction of the tension field exhibit better
130 performance.

131 Use of CFRP in laminating steel plates was initially investigated by Hatami and Rahai
132 [19]. They concluded that HSW with CFRP/steel infill plates in comparison with steel shear
133 walls have higher energy dissipation and enhanced elastic stiffness and shear capacity [19].
134 Petkune et al. [20] compared the behaviour of both GFRP/steel and CFRP/steel infill plates
135 in HSW design within steel boundary elements. Further, more detailed investigation of the
136 role of boundary conditions [21] in the usage of CFRP or GFRP as an element in hybrid infill
137 plates was presented.

138 Initial steps in the application of infrared thermography (IRT) for detecting
139 delamination between GFRP and steel in hybrid infill plates are reported in [17]. Petkune et
140 al. [22, 23] have extended this work for detection of delamination in hybrid steel/FRP infill
141 plates using IRT.

142 **2.3 Structural repair of SSW and HSW**

143 Limited studies are available on the structural repair and strengthening of the
144 damaged SSWs to recover their initial capacity after earthquakes. Petkune et al. [24]
145 conducted experimental studies of damaged SSWs with retrofitting the columns and infill
146 plate with GFRP bi-directional fabric and concluded this method to be a suitable temporary
147 retrofitting solution. Load capacity of the retrofitted specimen is increased in comparison with
148 pristine SSW, but it is limited to applications subjected to small displacements. However,
149 more effective permanent strengthening is needed to ensure sufficient capacity and durability
150 after repair [24].

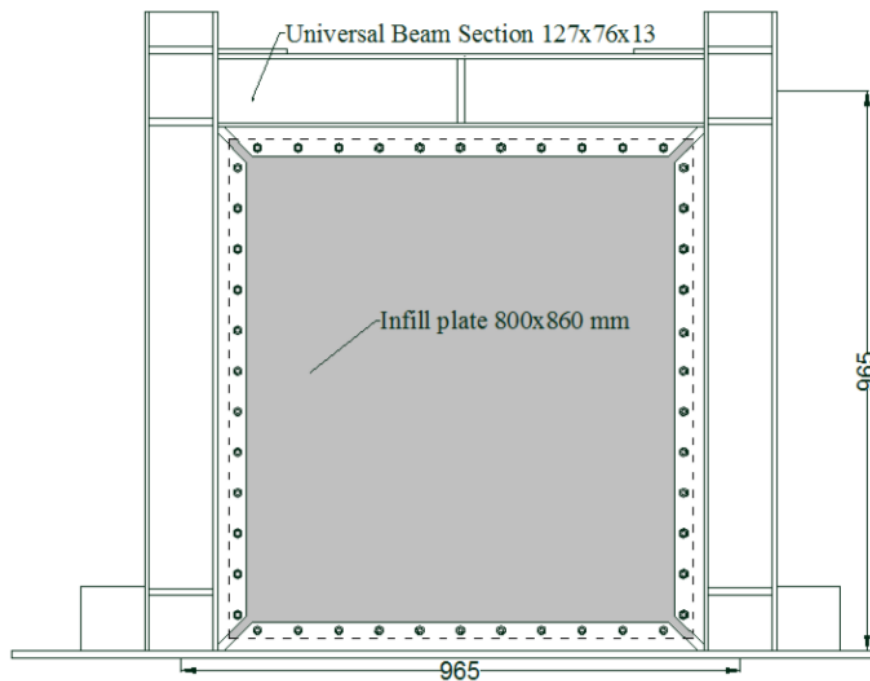
151 Both structural repair of the specimens and the development of new hybrid elements
152 indicate that simultaneous application of steel and FRP materials in seismic resistant

153 structures could be beneficial. This study aims to develop an effective structural repair
154 technique for SSW and HSW systems using FRP materials.

155 3 METHODOLOGY

156 3.1 Description of specimens

157 Shear wall specimens are scaled models with a height of 1025 mm and width of 1090
158 mm (see Figure 1). All specimens are made from steel frames and steel or hybrid infill plates.
159 Steel frame members consist of two columns and a beam, all of them made from UB 127 x
160 76 x 27 sections (S355 grade). The shear wall scaled models were designed at Kingston
161 University London and manufactured by Cannon Steels Ltd. Primary fish plates were welded
162 continuously to the steel frame.



163

164

Figure 1. Dimensions of shear wall specimens.

165 Two different groups of specimens were tested. In the first phase of the programme three
166 pristine specimens: steel shear wall (SSW-P), hybrid steel /CFRP shear wall (HSCSW-P)
167 and hybrid steel/GFRP shear wall (HSGSW-P) were tested. In the second phase of the work,
168 the tested specimens in the first phase were retrofitted and retested. These specimens are

169 identified as SSW-R, HSCSW-R and HSGSW-R. The structural repair of specimens in the
 170 second phase was undertaken by replacing the damaged infill plates with new infill plates of
 171 the same type, and strengthening the vertical steel frame elements with CFRP laminates and
 172 GFRP fabric. The pristine specimens are used as reference specimens to measure the scale
 173 of restoration of retrofitted specimens.

174

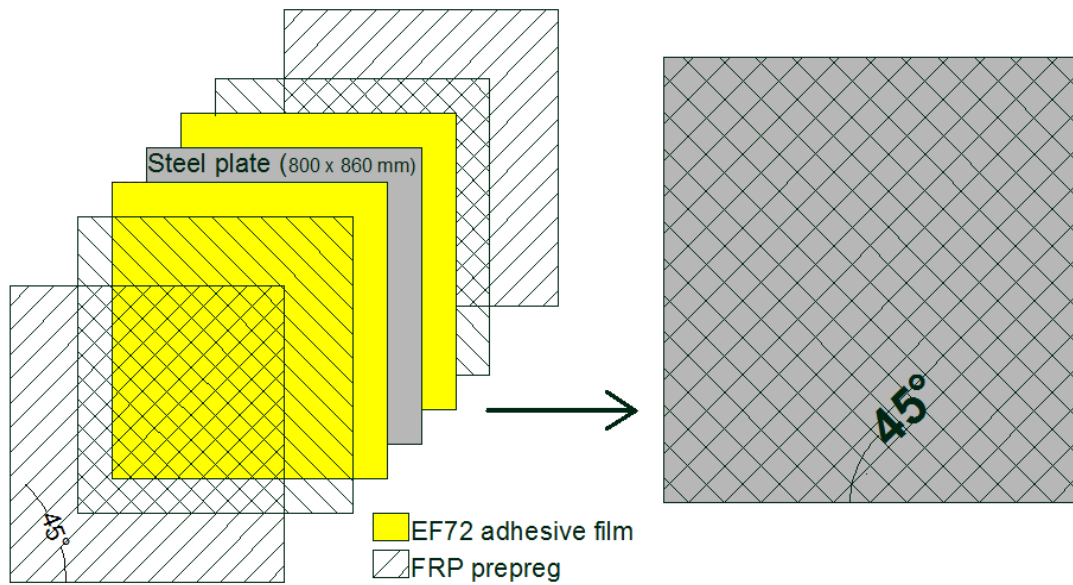
175 The specifications of all specimens are summarised in Table 1.

176 **Table 1.** Description of SSW and HSW specimens.

Name of the specimen	Labels	Stacking sequence of the infill plate	Total thicknesses of the infill plate, mm
Steel Shear Wall	SSW-P	Steel [S]	0.80
Retrofitted Steel Shear Wall	SSW-R	Steel [S]	1.40
Hybrid Steel/CFRP Shear Wall	HSCSW-P	[+45/-45/A/S/A/-45/+45]	1.70
Retrofitted Hybrid Steel/CFRP Shear Wall	HSCSW-R	[+45/-45/A/S/A/-45/+45]	1.70
Hybrid Steel/GFRP Shear Wall	HSGSW-P	[+45/-45/A/S/A/-45/+45]	2.40
Retrofitted Hybrid Steel/GFRP Shear Wall	HSGSW-R	[+45/-45/A/S/A/-45/+45]	2.40

177 Note: A- adhesive film (EF72)

178 For the steel shear wall (SSW-P) specimen, an infill plate of a 0.8 mm thick from steel
 179 grade S275 was used. In the hybrid specimens the same steel frames were used but the infill
 180 plates were prepared by symmetrically laminating a steel plate (0.8 mm thick) with two layers
 181 of unidirectional (UD) FRP prepreg material on both sides (Figure 2). Unidirectional fibre
 182 orientations were placed at $\pm 45^\circ$ relative to the loading direction. The use of the UD FRP
 183 prepreg allowed the customization of the infill plates according to design requirement in
 184 terms of the fibre orientation and number of FRP layers.



185

186

Figure 2. Design specification for hybrid specimens.

187

188

189

190

191

192

193

For HSCSW-P and HSCSW-R, unidirectional CFRP prepreg type Medium Temperature Molding MTM 28-1 series (produced by Cytec Solvay Group) was laminated on both sides of the steel infill plate. For HSGSW-P and HSGSW-R, unidirectional GFRP prepreg with epoxy resin E722-02 (produced by TenCate Advanced Composites Ltd) was laminated on the both sides of the steel infill plate. The mechanical properties of these prepreg are summarised in Table 2.

Table 2. Mechanical properties of the FRP materials.

	Unidirectional CFRP type MTM 28-1 series prepreg (Cytec Solvay Group)	Unidirectional GFRP prepreg E722-02 (produced by TenCate Advanced Composites Ltd)
Young's Modulus E_{11} , GPa	140	41
Young's Modulus E_{22} , GPa	8.5	10.5
Shear Modulus G_{12} , GPa	5.8	3.3
Poisson's ratio ν_{12}	0.319	0.311

194

195

196

197

198

For the preparation of hybrid infill plate, FRP layers were laminated according to the manufacturer's recommendations. The infill plates were prepared by thoroughly cleaning the steel plate with sand paper followed by acetone. EF72 adhesive film (manufactured by TenCate Advanced Composites Ltd) with area weight of 100 g/m^2 was placed between the

199 steel plate and FRP prepreg to create a strong bond between FRP laminate and core steel
200 infill plate. The additional adhesive film delays the delamination of FRP prepreg during cyclic
201 loading. Then FRP prepregs were laid according to the design specifications with fibre
202 orientations as indicated in Table 1. The specimen was vacuum bagged and cured inside an
203 oven under vacuum (Figure 3a). The curing temperature increased at a rate of 3°C per
204 minute until 120°C and an even pressure up to 980 mbar was applied to the laminate by
205 using a vacuum pump (Figure 3b). Then the temperature was kept constant at 120°C for 1
206 hour and finally the temperature decreased to 60°C during the cooling down cycle and the
207 sample was then left to cool to room temperature outside the oven.

208

209

210

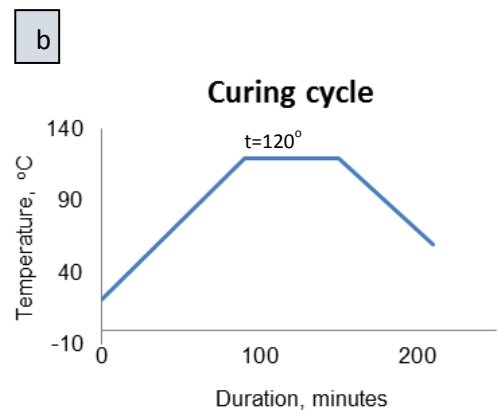
211

212

213

214

215



216

Figure 3. a) oven/vacuum curing of the plate b) curing cycle.

217

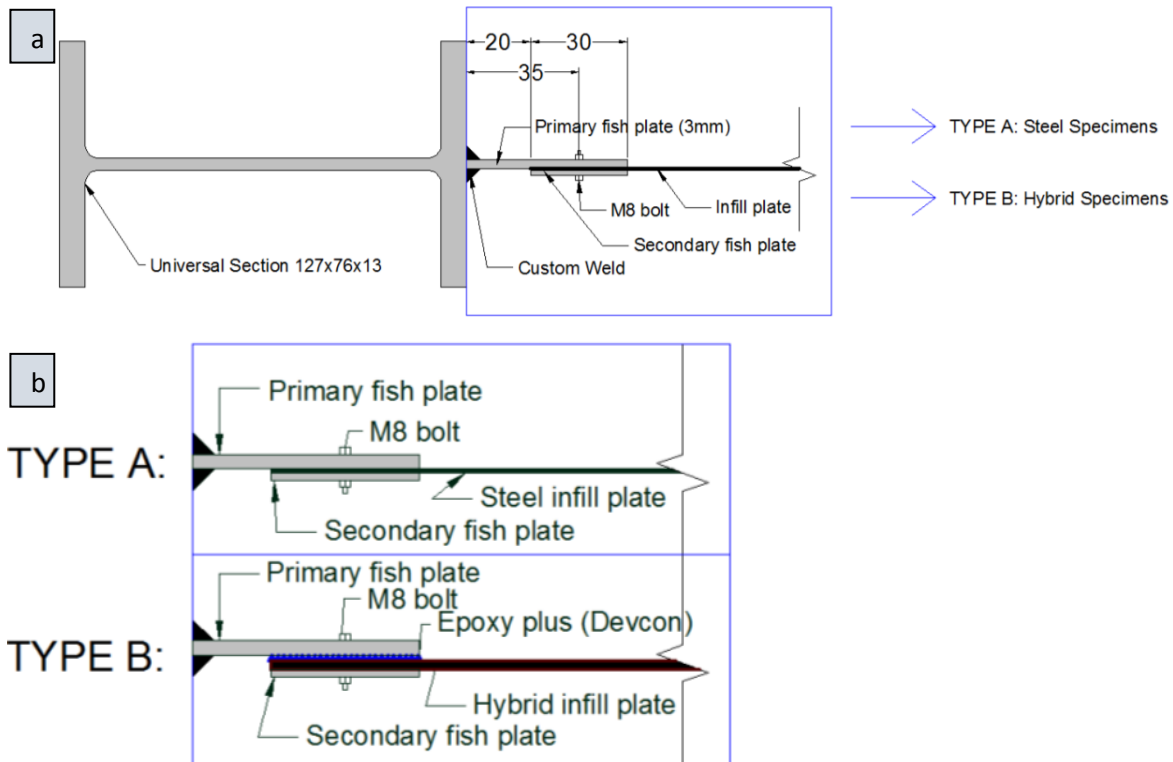
218

219

220

221

In the steel shear wall specimens, infill plates were bolted to the fish plates (Figure 4a). In the hybrid specimens, in addition to bolts a Devcon epoxy plus adhesive (manufactured by ITW Polymers Adhesives) with a shear strength of 20 MPa was used (Figure 4b) to compensate a relatively weak connection between FRP surface of infill plate and steel surface of fish plates due to the lower coefficient of friction.



222

223

224 **Figure 4.** Connection between fish plates and infill plate a) top view of I-beam section and
 225 infill plate b) types of connections in steel and hybrid infill plates.

226

227 **3.2 Retrofitting of tested specimens**

228 The three specimens from the first phase were tested under quasi-static cyclic loading up
 229 to a significant level of damage as a result of high in-plane displacement at the top of the
 230 frame. For the second phase, these specimens were retrofitted and indicated as SSW-R,
 231 HSCSW-R and HSGSW-R.

232 **Table 3.** Properties of the FRP materials used for retrofitting of shear walls.

Properties of CFRP laminates [25]		Properties of GFRP fabric [26]	
Density, g/cm ³	1.7	Fibre density, kg/cm ³	2.6
Fibre content, v _f %	70	Area weight, g/cm ²	350
Elastic modulus E _f , GPa	165+	Modulus of elasticity E _{cu} , GPa	65+
Tensile strength f, MPa	2800+	Tensile strength f _{cu} , MPa	2000+

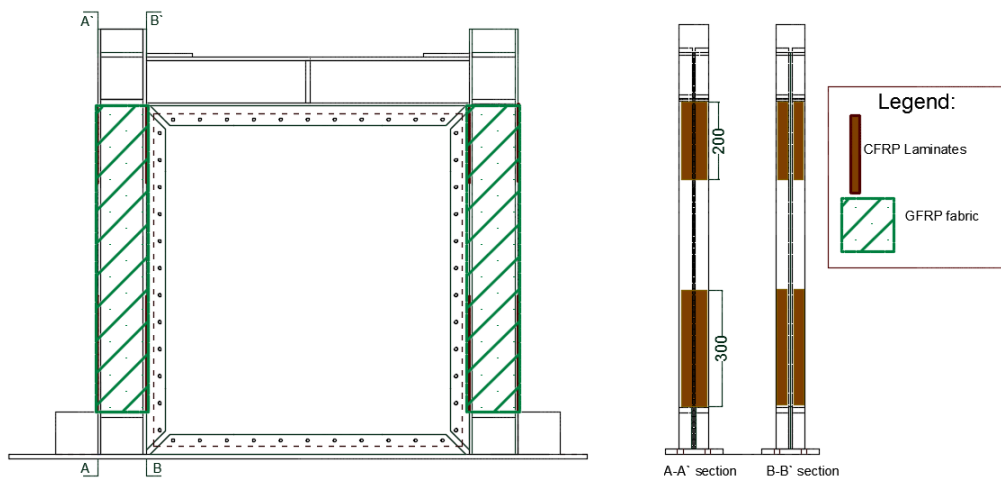
233

234 The procedure for repairing the original specimens was as following:

- 235
- Removal of damaged infill plates
 - Strengthening of the frame with CFRP laminates
- 236

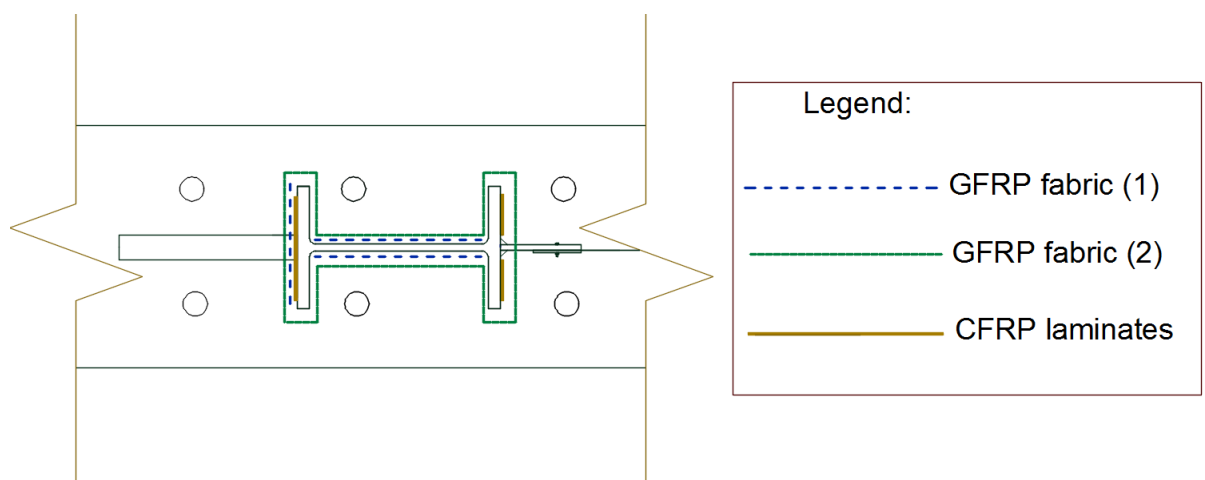
- 237 • Wrapping of the frame with GFRP fabric
- 238 • Replacement of infill plate with a new one

239 Due to the lack of visual damage in the horizontal members of the frame, Weber
240 CFRP S&P CFK 150/2000 unidirectional laminates 1.2 mm thick [25] were attached to the
241 vertical boundary elements only, aiming to cover the area where plastic hinges were formed
242 after previous loading in phase one. The plastic hinges were developed at the bottom and
243 top sections of the vertical elements. The repairs were undertaken by firstly removing the
244 paint with a mechanical wire brush in areas where CFRP laminates and GFRP fabric were
245 planned to be applied. This improved the bonding between the steel and the FRP
246 composites. Then the frame was cleaned with white spirit to remove dust and oil. CFRP
247 laminates were bonded to the frame (Figure 5) with a moisture-tolerant structural adhesive
248 from “Weber”. The adhesive has two parts: bisphenol epoxy resin and polyamine hardener,
249 which were mixed with a mass ratio of 2.4:1 according to the supplier’s instructions. The
250 adhesive thickness was approximately 3 mm. The A-A section of the I-beam was
251 strengthened with 300 mm (bottom part) and 200 mm (top part) long and 65 mm wide Weber
252 CFRP laminates. The B-B section of I-beam was strengthened with 25 mm wide CFRP
253 laminates with the same lengths as for A-A section. The minimised area of the application of
254 CFRP laminates is adopted from the point of view of more economical strengthening of
255 whole building. In general case if the economy of CFRP laminates is not significant, their
256 application over the whole vertical surface could be beneficial in aspect of improving of their
257 anchorage. Mechanical properties of FRP materials used for retrofitting are tabulated in
258 Table 3.



259
 260 **Figure 5.** Retrofitting scheme: position of CFRP laminates on shear wall columns (A-A and
 261 B-B sections)

262 After curing of CFRP laminates and adhesive bond, Weber bi-directional woven GFRP
 263 wrapping [26] was laid on the frame (Figure 6) using a mixture of epoxy resin and hardener
 264 (2:1 by mass ratio). GFRP fabric was applied in two stages: firstly GFRP fabric was applied
 265 along the web of the I-beam and along the A-A section of the I-beam as the first layer to
 266 allow for proper attachment of the fabric in the areas of internal corners of the section. Then
 267 GFRP was wrapped around the whole surface of the columns (Figure 6) as the second layer
 268 of GFRP for the areas where first layer is applied. Due to the shape of the I-beam, double
 269 wrapping allowed avoidance of “air pockets” in the corners of the section.

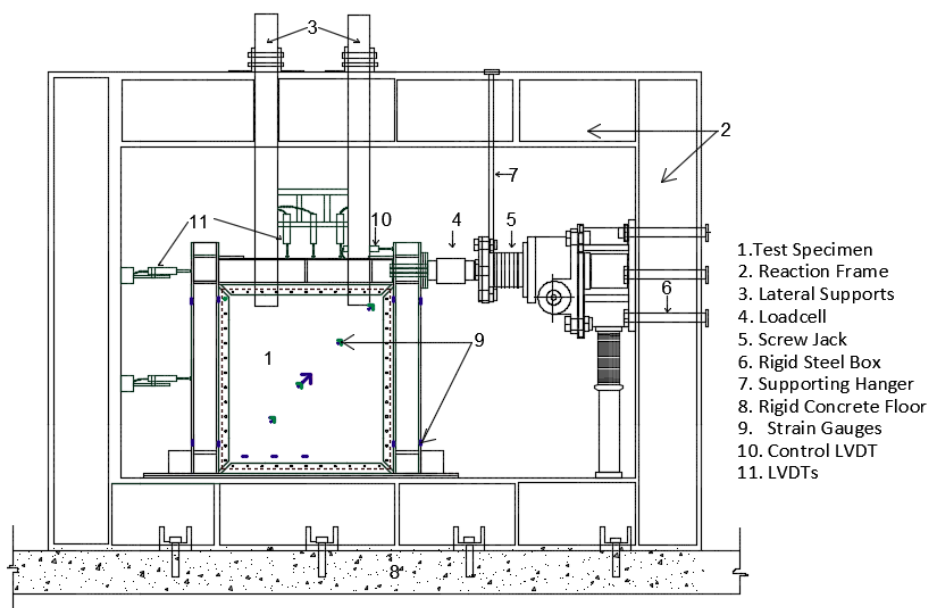


270
 271 **Figure 6.** Positioning of CFRP laminates and GFRP fabric on the plan view of the frame

272 The damaged 0.8 mm thick infill plate from the steel shear wall specimen was replaced
 273 with a steel infill plate of thickness of 1.4 mm. The choice of a higher thickness of steel infill
 274 plate in this case was due to strengthening considerations. Hybrid specimens were replaced
 275 with infill plates with the same steel plate and FRP design specifications as in the pristine
 276 specimens.

277 3.3 Scaled shear wall test set-up and protocol

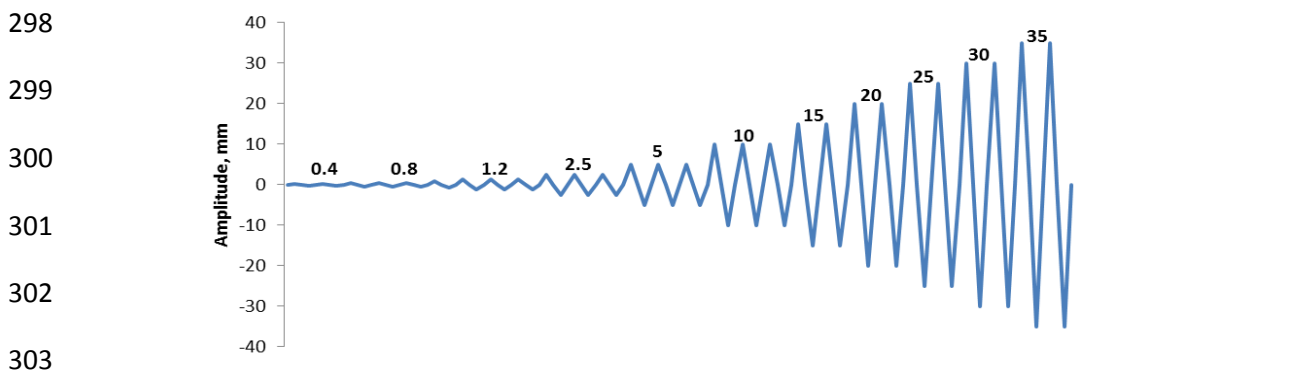
278 The scaled shear wall test set-up is shown in Figure 7. The testing rig consists of the
 279 reaction frame, loading system and lateral supports. Each of the test specimens was fixed to
 280 the bottom part of the reaction frame via high strength bolts and clamps, with lateral supports
 281 preventing out-of-plane buckling of the specimen during testing. Shear wall specimens were
 282 tested under quasi-static cyclic displacement controlled loading in the in-plane horizontal
 283 direction. The loading system consisted of a screw jack, electric motor, gear box and inverter.
 284 The applied in-plane force was measured with a 500 kN load cell. Linear variable differential
 285 transformers (LVDTs) were used to record displacements. The control LVDT used for
 286 measuring displacements in Figures 12, 13 and 14 is indicated as No.10 in Figure 7. Strain
 287 gauges were used to record local strain in the plate.



288
 289

Figure 7. Test set-up for shear wall specimens.

290 The testing procedure was according to ATC-24 protocol from Applied Technical
291 Council [27]. Figure 8 shows cyclic sinusoidal loading designed for these specific types of
292 specimens and applied for a range of different displacement amplitudes varying from 0.4 mm
293 to 35 mm displacement. The rate of the applying displacement varied from 0.05 mm/min
294 between 0.4 mm and 10 mm displacements to around 2.2 mm/min between 10 mm and 35
295 mm displacements. Initially, three cycles at each amplitude were applied, and then above 15
296 mm displacement the number of cycles was decreased to two cycles per amplitude
297 according to the ATC-24 protocol.



304 **Figure 8.** Quasi-static cyclic displacement control loading according to ATC-24 protocol.

305 4 RESULTS AND ANALYSIS

306 4.1 Behaviour of pristine and retrofitted specimens

307 In this section the behaviours of the pristine and retrofitted specimens are discussed
308 including the information about failure mechanisms occurring during the tests. Any changes
309 to infill plates including visual appearance and progression of delamination between FRP
310 layers and steel infill plate, plastic hinges in columns and delamination of the CFRP
311 laminates and GFRP fabric from columns are closely monitored and reported. Furthermore,
312 damage between the infill plate and boundary elements is investigated.

313

314

315

316 **4.1.1 Behaviour of pristine SSW-1 and retrofitted SSW-2 specimens**

317 The pristine steel shear wall specimen SSW-P (Figure 9a) was loaded up to 35 mm
318 displacement. The first signs of buckling of the infill plate occurred at 1.2 mm displacement,
319 which did not fully recover after the end of the 2.5 mm loading cycle. The number and
320 amplitude of diagonal tension field waves were increased at higher displacements. At
321 displacements higher than 10 mm, enlargement of holes around bolts in the connections
322 between fish plates and infill plates started, which led to the yielding of the steel infill plate
323 and its tearing around these areas. In addition sliding of the infill plate progressed with the
324 increase of the displacements. Development of the plastic hinges at the bottom of the
325 columns of the steel frame was noticed at displacements above 15 mm and at the top of the
326 columns with 30 mm displacement. The initial pinching of the infill plate started at a
327 displacement of 15 mm, which further progressed to development of small holes at
328 displacements higher than 30 mm. The final failure of the steel shear wall specimen occurred
329 through the development of the plastic hinges around the bottom and top areas of the
330 column and tearing of the steel plate around bolt holes.



331
332 (a)

(b)

333 **Figure 9.** a) Pristine SSW-P and b) retrofitted SSW-R specimens after loaded to 35 mm
334 displacement.

335 In the retrofitted SSW-P specimen (Figure 9b) visible diagonal tension field
336 development started at a displacement of 3.5 mm in both directions of loading and produced

337 wave-type deformations, which did not fully recover after the end of 3.5 mm loading cycle.
338 Further development of the diagonal tension field was recorded with an increase of the
339 applied displacement. At a displacement of 10 mm, buckling of the primary fish plate
340 occurred where the diagonal tension field waves developed. At displacements above 15 mm,
341 plastic hinges at the bottom of the columns were developed, which led to the development of
342 delamination in GFRP fabric. Sliding between primary fish plates and infill plates was initially
343 recorded for the top and side boundary elements. At 25 mm displacement, development of
344 debonding of the CFRP laminates attached to the top of the columns occurred. With the
345 increase of the loading displacement to 30 mm, further development of the diagonal tension
346 field led to pinching in the centre of the plate with the appearance of small holes. At 35 mm
347 displacement of loading, further progression of the debonding for all CFRP laminates and
348 delamination for GFRP fabric occurred in the lower section of the columns.

349 **4.1.2 Behaviour of pristine HSCSW-P and retrofitted HSCSW-R specimens**

350 In pristine HSCSW-P specimen (Figure 10a) the first sign of buckling of the infill plate
351 through the development of wave-type deformation was noticed at 1.2 mm displacement,
352 which did not recover fully at the end of the applied 2.5 mm displacement cycle.
353 Delamination between FRP and steel plate started in the top corners of the plate along
354 diagonal tension field action, which developed at 10 mm displacement and grew further at
355 higher applied displacement. Sliding and tearing in the connections between fish plates and
356 infill plate started at displacements higher than 15 mm, cracks in the adhesive layer and
357 sliding increased at higher displacement. At 25 mm loading, infill plate had snapped in the
358 top corners near primary fish plates where diagonal tension field was developed with
359 occurrence of holes and delamination of the FRP; elongated bolt holes were visible at
360 displacement of 30 mm. Considerable delamination between CFRP layers and steel plate
361 along the full length of diagonal tension field action and in the corners has been noticed for
362 HSCSW-P at displacement above 25 mm. The specimen was tested up to 30 mm
363 displacement loading.



364
365

(a)

(b)

366 **Figure 10.** a) Pristine HSCSW-P specimen after loaded to 30 mm displacement b) retrofitted
367 HSCSW-R specimens after loaded to 35 mm displacement.

368 In retrofitted HSCSW-R specimen (Figure 10b), visible diagonal tension field
369 development started at the displacement of 2.5 mm, the resulting lateral deformations did not
370 fully recover after the end of 2.5 mm loading cycle. Further diagonal tension field waves both
371 in size and number developed with increase of the loading displacement. Other visible
372 changes to the frame and infill plate were noticed at 10 mm displacement, such as cracking
373 in CFRP layers along diagonal tension field action recorded in both directions, which was
374 increased at higher levels of the loading displacement. The integrity of the bond in the
375 connection between fish plates and infill plate was compromised at 15 mm displacement and
376 further cracking in the adhesive developed with increase of the displacements. At 20 mm
377 displacement, cracks in the CFRP layers developed at the bottom part of the infill plate. At 25
378 mm displacement plastic hinges developed at the bottom of the columns. Similar snapping of
379 the infill plate occurred in the top corners near fish plates, as it occurred in pristine HSCSW-P
380 specimen. Further damage to the connection between infill plates and fish plates occurred at
381 30 mm displacement, when bolt holes elongations became visible. The test was terminated
382 at 35 mm displacement.

383
384
385

386 **4.1.3 Behaviour of pristine HSGSW-P and retrofitted HSGSW-R specimens**

387 In pristine HSGSW-P specimen (Figure 11a), visible diagonal tension field
388 development started at the displacement of 1.2 mm in both directions, deformations did not
389 fully recover after the end of 2.5 mm loading cycle. At displacement higher than 10 mm,
390 development of tension field residual deformations in both directions led to the delamination
391 of GFRP fabric from steel plate in the top corners of the infill plate. With further loading of the
392 specimen, delamination along diagonal tension field action increased. At 15 mm
393 displacement, cracking in the adhesive layer between fish plates and the infill plate was
394 noticed. First signs of the development of the plastic hinges at the bottom of columns were
395 recorded at 20 mm displacement. At higher displacement delamination was propagated
396 further, however the extent of delamination was smaller compared to pristine HSCSW-P
397 specimen at the same level of loading. At 30 mm displacement, the top corners in the infill
398 plate around fish plates snapped and the elongations of bolt holes of the infill plate became
399 visible. The specimen was tested to 30 mm displacement loading.



400
401 **(a)**

(b)

402 **Figure 11.** a) Pristine HSGSW-P specimen after loaded to 30 mm displacement b) retrofitted
403 HSGSW-R specimens after loaded to 35 mm displacement.

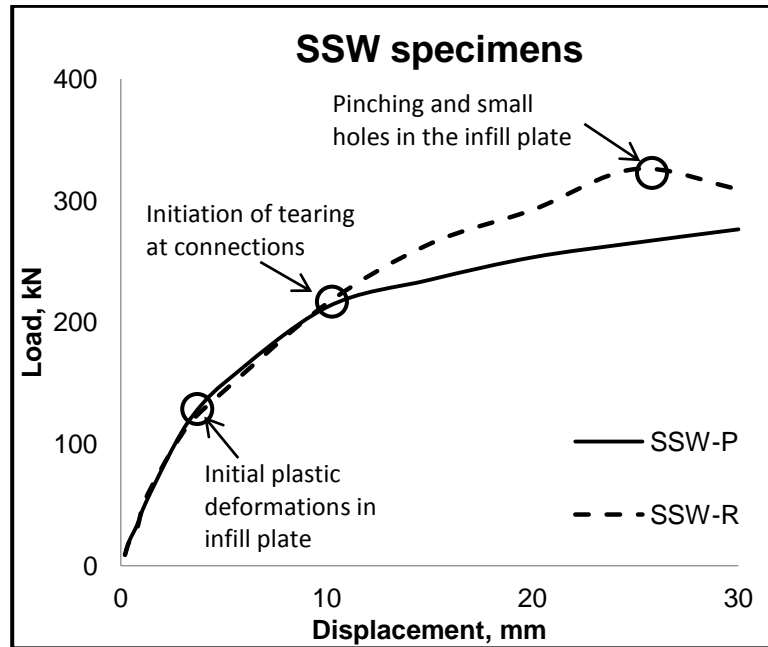
404 In retrofitted HSGSW-R specimen (Figure 11b), diagonal tension field action became
405 visible at 2.5 mm displacement, which did not fully recover at the end of the loading cycle.
406 First sign of cracking in the adhesive layer between fish plates and infill plate was noticed at

407 the displacement of 10 mm. Delamination of the GFRP layer from steel infill plate started at
408 displacement loading of 15 mm at the top corners. Development of the plastic hinges at the
409 bottom of the columns was noticed at 20 mm displacement, which led to the debonding of
410 the GFRP fabric from the columns. Snapping of the infill plate in the top corners occurred at
411 the same level of displacement of 30 mm as in the pristine HSGSW-P specimen. At 30 mm
412 displacement, plastic hinges were developed at top of the column; it also led to the
413 debonding of the CFRP laminates around the top sections of the columns. Additionally crack
414 in the connection between beam and column appeared. As the crack further progressed, the
415 test was terminated at the end of first cycle of 35 mm displacement. GFRP delamination area
416 from steel infill plate was smaller in comparison with pristine HSGSW-P specimen.

417 **4.2 Load - displacement results**

418 The load-displacement behaviours of pristine and retrofitted specimens are compared
419 in Figures 12, 13 and 14 to investigate the opportunity for effective structural repair of steel
420 and hybrid shear wall systems after they were subjected to seismic loading. Loads were
421 calculated by taking the average from the extreme values of the cycles at the same
422 displacement amplitude. The presented diagrams in Figures 12, 13 and 14 is an envelope
423 from those average values.

424 Up to 10 mm displacements, for SSW-P and SSW-R specimens (Figure 12) the load
425 values for corresponding displacements are approximately the same. The highest difference
426 of 22% was recorded at 25 mm displacement in load values in favour of retrofitted specimen.
427 Maximum load for the whole range of displacements for SSW-P was 285 kN and for SSW2
428 was 336 kN.

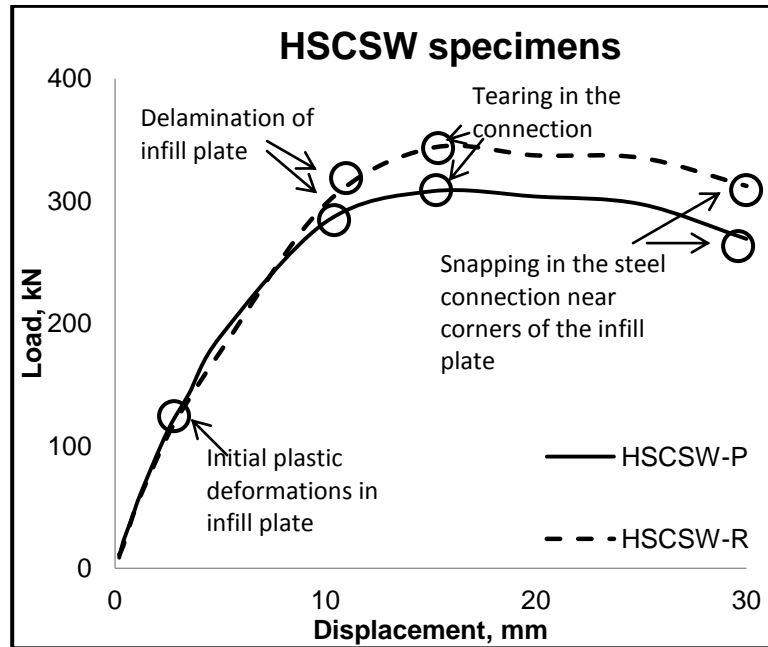


429

430 **Figure 12.** Load-displacement results for pristine SSW-P and retrofitted SSW-R specimens.

431

432 For HSCSW-P and HSCSW-R specimens (Figure 13), load values are nearly the
 433 same up to 7 mm displacement. In retrofitted HSCSW-R specimen larger increase in load
 434 was recorded for displacements between 7 mm and 15 mm displacements compared with
 435 HSCSW-P specimen. Above 15 mm displacement, load values was dropping for both
 436 specimens, however load values for retrofitted specimens were more than 10% higher
 437 compared to HSCSW-P specimen. HSCSW-R specimen achieved higher ultimate load in
 438 comparison with pristine HSCSW-P specimen, the difference in the ultimate load was
 recorded as 11% at 15 mm displacement.



439

440 **Figure 13.** Load-displacement results for pristine HSCSW-P and retrofitted HSCSW-R

441

specimens.

442

443

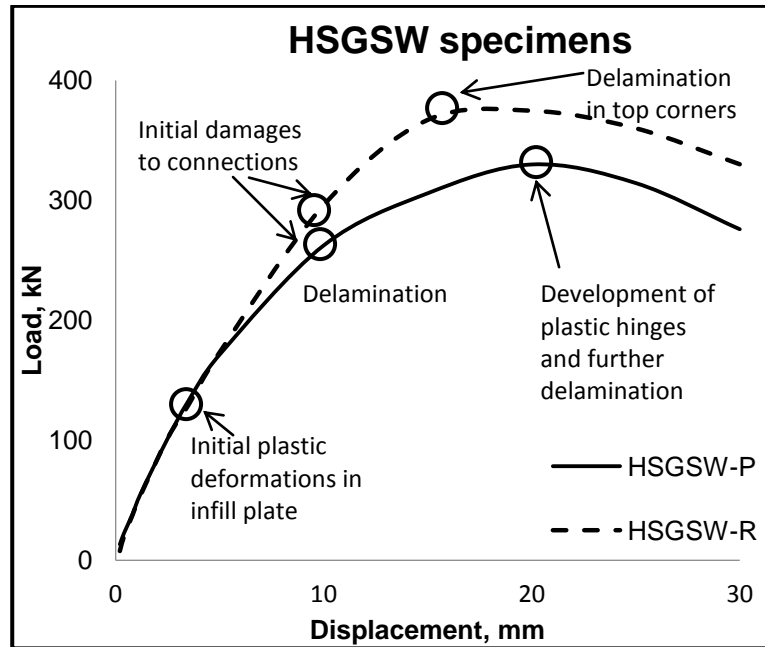
444

445

446

447

For HSGSW-P and HSGSW-R specimens (Figure 14) load value were approximately the same up to 5 mm displacement. At displacements between 5 mm and 15 mm, load values were higher for retrofitted HSGSW-R specimen in comparison with HSGSW-P. The highest load increase of 20% was recorded at 15 mm and at 30 mm displacements compared to pristine HSGSW-P specimen. The difference in ultimate load between retrofitted HSGSW-R and pristine HSGSW-P specimens was 14%.

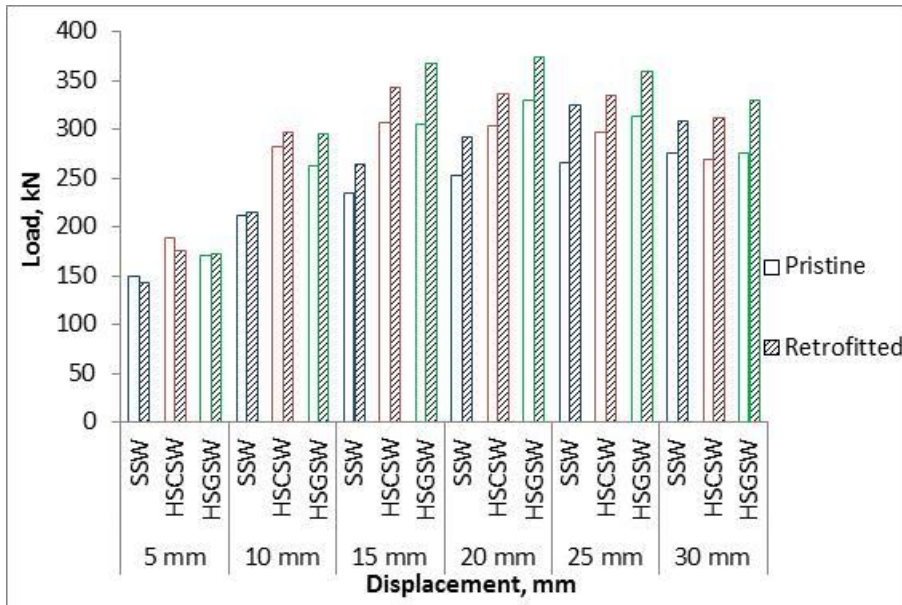


448

449 **Figure 14.** Load-displacement results for pristine HSGSW-P and retrofitted HSGSW-
 450 specimens.

451 For all types of the specimens, structural repair discussed above gave better results
 452 in respect of load values, ultimate load values and energy dissipation than the pristine
 453 specimens in the interval between 10 mm and 30 mm displacements.

454 Figure 15 compares load carrying capacity of pristine and retrofitted specimens
 455 starting at 5 mm displacement loading. From the behaviour of these two groups of
 456 specimens, it is noted that pristine and retrofitted hybrid carbon and hybrid glass have higher
 457 loading capacity than SSW specimens at every level of displacement loading. At 30 mm
 458 applied displacement due to significant delamination of FRP from infill plates in the direction
 459 of the tension field action, the behaviour of HSWs and SSW are nearly the same. Petkune et
 460 al. stated [20] that the use of the hybrid infill plates improves ultimate load values
 461 significantly. The same pattern of higher load carrying capacity for HSW specimens
 462 compared to SSW specimen was noted for retrofitted specimens.



463
464 **Figure 15.** Comparison of the load-displacement results of different shear wall
465 systems.

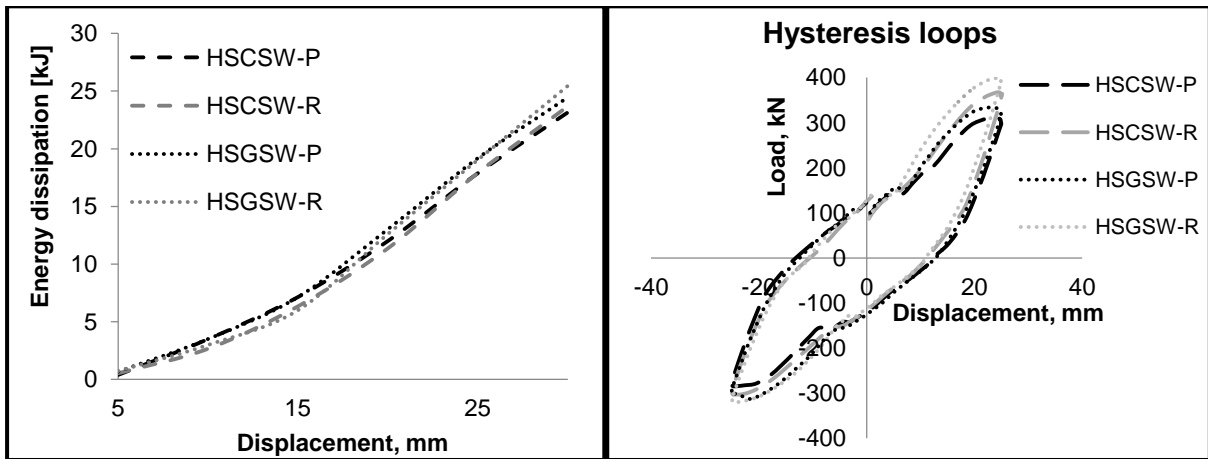
466 4.3 Energy dissipation in different types of shear wall specimens

467 Figure 16a shows energy dissipation for pristine and retrofitted specimens SSW,
468 HSCSW and HSGSW at different stages of cyclic loading. The energy dissipation was
469 calculated from measuring the area within all applied hysteresis loops. An example of the
470 hysteresis loop for hybrid carbon and hybrid glass specimens at 25 mm displacement is
471 shown in Figure 16b.

472 In the retrofitted SSW-R specimen energy dissipation relative to the pristine specimen
473 is higher between 10 mm and 30 mm displacement, difference in values reaching 1.418 kJ at
474 30 mm displacement mainly due to increased thickness of the infill plate.

475 For hybrid specimens, energy dissipation in pristine and retrofitted ones were
476 approximately the same; the biggest decrease of energy dissipation around 0.6 kJ for
477 retrofitted specimen in comparison with pristine specimen was recorded at 15 mm
478 displacements. Both retrofitted hybrid specimens had an increase in energy dissipation at 30
479 mm displacement, retrofitted HSCSW-R had 0.53 kJ increase and retrofitted HSGSW-R had
480 an increase of 0.982 kJ relative to SSW specimen.

481



482

483

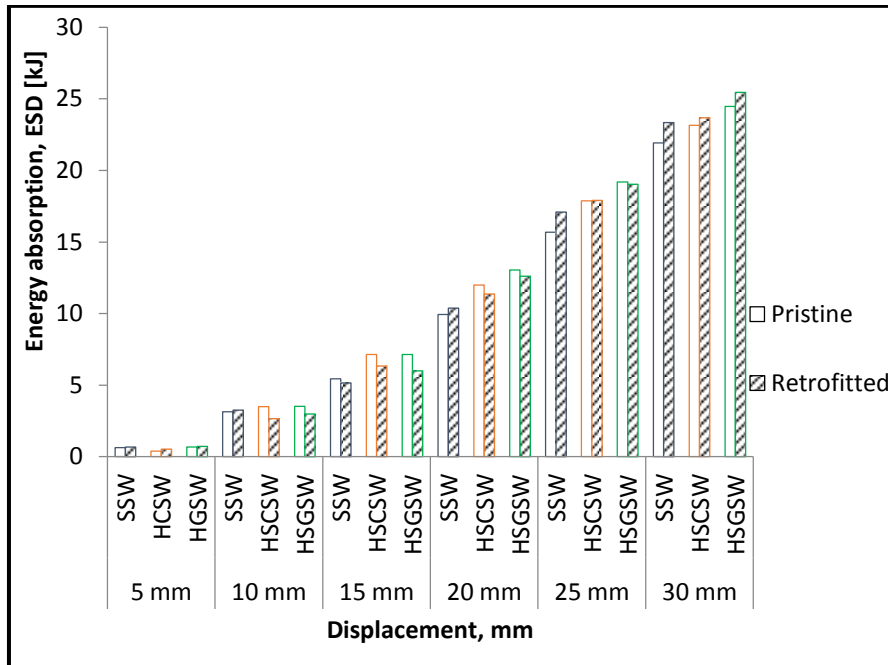
(a)

(b)

484 **Figure 16.** Energy dissipation in hybrid specimens: a) energy dissipation between 5mm and
485 30 mm b) hysteresis loops for hybrid specimens at 1st cycle of 25 mm displacement loading.

486 The differences in energy dissipation values for all specimens at different stages of
487 loading are summarised in Figure 17. Energy dissipation increases continuously from 5 mm
488 to 30 mm displacement in all specimens. Previous studies [20] showed that energy
489 dissipation in pristine hybrid specimens is higher than in steel specimens. The same
490 tendency has been observed for retrofitted specimens between 15 mm and 30 mm
491 displacements loading, and the highest result is achieved in retrofitted HSGSW-R specimen.

492



493

494 **Figure 17.** Comparison of energy dissipation in different types of shear wall specimens.

495 **6 CONCLUSIONS**

496 In this work scaled models of pristine steel and hybrid FRP shear walls were tested and
 497 after structural repair of the columns with CFRP laminates and GFRP fabric and replacement
 498 of the infill plates with new ones, retrofitted specimens were retested. From the test results
 499 the following conclusions can be made:

- 500 • Hybrid steel/CFRP and steel/GFRP shear walls have higher ultimate load in
 501 comparison with steel shear wall system within the applied levels of loading for both
 502 groups of tested specimens.
- 503 • Using the structural repair procedure outlined in the paper, resulted in higher ultimate
 504 load in retrofitted samples in comparison with pristine specimens.
- 505 • After retrofitting of the hybrid shear walls, the increases of load values are up to 16%
 506 higher for HSCSW and up to 20% higher for HSGSW. Corresponding increases of the
 507 ultimate load are 11% for HSCSW and 14% for HSGSW specimens.

- 508 • The energy dissipation of retrofitted specimens is very close to energy dissipation of
509 the pristine specimens. The differences for cumulative energy dissipation between
510 them during the full spectrum of loading are less than 10%.

511 In summary it has been shown that the proposed methodology for the retrofitting of damaged
512 shear walls by bonding FRP materials to the frame and replacement of the infill plate is
513 effective for all three configurations of specimens and the restored shear wall performance is
514 as good as the pristine one.

515

516 **Acknowledgement**

517 The authors are grateful for the financial support from Kingston University London and would
518 like to express gratitude to lab technicians in Structural, Composite and Materials
519 Laboratories at Kingston University.

520

521

522

523 **REFERENCES**

524

- [1] T. Roberts, "Seismic resistance of steel plate shear walls, *Engineering Structures*," vol. 17, no. 5, pp. 344-351, 1995.
- [2] J. W. Berman and M. Bruneau, "Experimental investigation of light-gauge steel plate shear walls," *J. Struct. Eng.*, vol. 131, no. 2, p. 259–267, 2005.
- [3] A. Rahai and M. Alipour, "Behavior and Characteristics of Innovative Composite Plate Shear Walls," *Procedia Engineering*, vol. 14, pp. 3205-3212, 2011.
- [4] S. Rizkalla, M. Dawood and D. Schnerch, "Development of a carbon fiber reinforced polymer system for strengthening steel structures," *Composites: Part A*, vol. 39, pp. 388-397, 2008.
- [5] J. Teng, T. Yu and D. Fernando, "Strengthening of steel structures with fiber-reinforced polymer composites," *Journal of Construction Steel Research*, vol. 78, pp. 131-143, 2012.
- [6] X.-L. Zhao and L. Zhang, "State-of-the-art review on FRP strengthened steel structures," *Engineering Structures*, vol. 29, pp. 1808-1823, 2007.
- [7] A. Harries, A. Peck and E. Abraham, "Enhancing stability of structural steel sections using FRP," *Thin-Walled Structures*, vol. 47, pp. 1092-1101, 2009.
- [8] S. El-Tawil, E. Ekiz, S. Goel and S.-H. Chao, "Retraining local and global buckling behavior of steel plastic hinges using CFRP," *Journal of Construction Steel Research*, vol. 67, p. 261–269, 2011.
- [9] D. Schnerch and Rizkalla S., "Flexural strengthening of steel bridges with high modulus CFRP strips," *Journal of Bridge Engineering*, vol. 13, no. 2, p. 192–201, 2008.
- [10] E. Ghafoori, M. Motavalli, X.-L. Zhao, A. Nussbaumer and M. Fontana, "Fatigue design criteria for strengthening metallic beams with bonded CFRP plates," *Engineering Structures*, vol. 101, pp. 542-557, 2015.
- [11] Q. Yu, T. Chen, X. Gu, X. Zhao and Z. Xioa, "Fatigue behaviour of CFRP strengthened steel plates with different degrees of damage," *Thin-Walled Structures*, vol. 69, pp. 10-17, 2013.
- [12] M. Lesani, M. Bahaari and M. Shokrieh, "FRP wrapping for the rehabilitation of Circular Hollow Section (CHS) tubular steel connections," *Thin-Walled Structures*, vol. 90, pp. 216-234, 2015.
- [13] T. Yu, Y. Hu and J. Teng, "FRP-confined circular concrete-filled steel tubular columns under cyclic axial compression," *Journal of Constructional Steel Research*, vol. 94, pp. 33-48, 2014.
- [14] J. Berman, O. Celik and M. Bruneau, "Comparing hysteretic behaviour of the light-gauge steel

-] plate shear walls and braced frames,” *Engineering Structures*, vol. 27, pp. 475-485, 2005.
- [15 C. Li, K. Tsai, J. Chang and C. Lin, “Cyclic Test of a Coupled Steel Plate Shear Wall Substructure.] The Twelfth East Asia-Pacific Conference on Structural Engineering and Construction,” *Procedia Engineering*, vol. 14, pp. 582-589, 2011.
- [16 M. Alinia and M. Dastfan, “Behaviour of thin steel plate shear walls regarding frame members,”] *Journal of Constructional Steel Research*, vol. 62, pp. 730-738, 2006.
- [17 A. Maleki, T. Donchev, H. Hadavinia and M. Limbachiya, “Improving the seismic resistance of] structure using FRP/steel shear walls,” in *Proceedings of 6th international Conference on Fiber Reinforced Polymer (FRP) Composites in Civil Engineering (CICE2012)*, Rome, Italy, 2012.
- [18 F. Nateghi-Alahi and M. Khazaei-Poul, “Experimental study of steel plate shear walls with the] infill plates strengthened by GFRP laminates,” *Journal of Construction Steel Research*, vol. 78, pp. 159-172, 2012.
- [19 F. Hatami, A. Ghamari and A. Rahai, “Investigating the properties of steel shear walls einforced] with Carbon Fiber Polymers (CFRP),” *Journal of Construction Steel Research*, vol. 70, pp. 36-42, 2012.
- [20 N. Petkune, T. Donchev, H. Hadavinia, M. Limbachiya and D. Wertheim, “Investigation of the] behaviour of hybrid steel and FRP shear walls,” in *Proceedings of 7th international Conference on Fiber Reinforced Polymer (FRP) Composites in Civil Engineering (CICE2014)*, Vancouver, Canada, 2014.
- [21 N. Petkune, T. Donchev, H. Hadavinia and M. Limbachiya, “Investigation in connections between] steel, composite and hybrid structural elements,” in *Proceedings of MCM-2014: Mechanics of composite materials conference*, Riga, Latvia, June 2014.
- [22 N. Petkune, T. Donchev, D. Wertheim, M. Limbachiya and H. Hadavinia, “Application of infrared] thermography for assessment of condition of structural element,” in *SMAR 2013: Second Conference on Smart Monitoring Assessment and Rehabilitation of Civil Structures*, Istanbul, Turkey., September 2013.
- [23 N. Petkune, T. Donchev, D. Wertheim, H. Hadavinia and M. Limbachiya, “The use of the IRT to] assess Steel and FRP hybrid elements,” in *SMAR 2015: Third Conference on Smart Monitoring Assessment and Rehabilitation of Civil Structures*, Antalya, Turkey, September 2015.
- [24 N. Petkune, T. Donchev, D. Petkova, H. Hadavinia, M. Limbachiya and Y. Hussein, “Opportunities] for strengthening of damaged steel shear walls,” in *Proceedings of Conference on Civil Engineering Infrastructure Cased on Polymer Composites (CECOM)*, Krakow, Poland, November

2012.

- [25 Weber, "Weber.Tec Force Carbon Plate," in *Retrieved from*
] http://www.netweber.co.uk/uploads/tx_weberproductpage/10.010_weber.tec_force_carbon_plate.pdf, July 2008, Available online.
- [26 Weber, "Weber.Tec force glass sheet," in *Retrieved from*
] http://www.netweber.co.uk/uploads/tx_weberproductpage/10.030_weber.tec_force_glass_sheet.pdf, July 2008, Available online.
- [27 ATC-24, "Guidelines for Seismic testing of components of steel structures," Report 24, Applied
] Technology Council, Redwood City, CA, 1992.

525

526